New Limit on Lorentz- and *CPT*-Violating Neutron Spin Interactions

J. M. Brown, S. J. Smullin, T. W. Kornack, and M. V. Romalis
Department of Physics, Princeton University, Princeton, New Jersey 08544
(Received 28 June 2010; published 5 October 2010)

We performed a search for neutron spin coupling to a Lorentz- and *CPT*-violating background field using a magnetometer with overlapping ensembles of K and ^{3}He atoms. The comagnetometer is mounted on a rotary platform for frequent reversal of its orientation. We measure sidereal oscillations in the signal to search for anomalous spin coupling of extra-solar origin. We determine the equatorial components of the background field interacting with the neutron spin to be $\tilde{b}_X^n = (0.1 \pm 1.6) \times 10^{-33}$ GeV and $\tilde{b}_Y^n = (2.5 \pm 1.6) \times 10^{-33}$ GeV, improving on the previous limit by a factor of 30. This measurement represents the highest energy resolution of any spin anisotropy experiment.

DOI: 10.1103/PhysRevLett.105.151604 PACS numbers: 11.30.Cp, 11.30.Er, 21.30.Cb, 32.30.Dx

Experimental searches for anomalous spin coupling to an anisotropy in space were first considered by Hughes [1] and Drever [2]. Since then, a number of such tests have been performed with electron and nuclear spins with increasing sensitivity [3–9]. There has been a resurgence of interest in these searches following the development of a general formalism for Lorentz and *CPT* violation called the standard model extension (SME) by Kostelecký [10]. The SME contains a number of possible terms that violate local Lorentz invariance by coupling to particle spin [11]. Furthermore, it has been shown that *CPT* violation necessarily leads to Lorentz violation [12], opening the possibility of *CPT* tests without the use of antiparticles. Anisotropic spin coupling appears in a number of Lorentz-violating models, for example, models with modified dispersion relationships at high energy [13], noncommutativity of space-time [14], and supersymmetric Lorentz violation [15]. This suggests that it is a rather general feature of Lorentz-violating theories.

The absolute energy sensitivity to anisotropic spin interactions is a good figure of merit for Lorentz and *CPT* tests within the SME. Previously, the most sensitive such test was performed with neutrons using a ^{3}He-^{129}Xe Zeeman maser [8]. Here, we use a K-^{3}He comagnetometer to reach 0.7 nHz energy resolution, improving the previous limit by a factor of 30. Existing limits on possible electron interactions [9] and the simple nuclear spin structure of ^{3}He [16] allow us to set clean limits on nuclear spin Lorentz violation, mostly sensitive to neutron interactions.

The K-^{3}He comagnetometer is similar to that described in [17,18] but is smaller in size. For this experiment the entire optical setup is operated in vacuum to reduce low frequency noise from air currents, and the apparatus is mounted on a rotary platform to reverse the direction of its sensitive axis every 22 seconds. We measure the sidereal oscillations of the signal to remove Earth-fixed backgrounds, such as the gyroscopic signal due to Earth's rotation.

The physics of the K-^{3}He comagnetometer has been described elsewhere [17,19,20]. Briefly, a circularly polarized laser optically pumps a high density K vapor. Spin-exchange collisions between K and ^{3}He atoms polarize ^{3}He spins. These overlapping spin ensembles are coupled via spin-exchange and their magnetic interaction. An applied B_z magnetic field parallel to the pump beam cancels the effective magnetic field experienced by K atoms due to nuclear spin magnetization of ^{3}He. As a result, the K magnetometer operates near zero field, where Zeeman resonance broadening due to spin-exchange collisions between alkali-metal atoms is eliminated [21]. At a particular value of the B_z field called the compensation point, the $\hat{x}$ polarization of K atoms has a particularly simple form, given to leading order by:

$$P_x^e = \frac{P_z^e \gamma_e}{R_{\mathrm{tot}}} \left(\beta_y^N - \beta_y^e + \frac{\Omega_y}{\gamma_N} \right). \tag{1}$$

Here, β_y^N and β_y^e describe the phenomenological magnetic-like fields in the $\hat{y}$ direction that couple only to the ^{3}He nucleus and K electrons, respectively. P_z^e and R_{tot} are the K electron spin polarization and relaxation rate, γ_e and γ_N are the gyromagnetic ratios for electrons and ^{3}He nuclei, respectively, and Ω_y is the rotation rate of the apparatus. Since K and ^{3}He atoms occupy the same volume, the comagnetometer is insensitive to ordinary magnetic fields ($\beta_y^N = \beta_y^e$), but retains sensitivity to anomalous interactions that do not scale with the magnetic moment.

The experimental setup is shown in Fig. 1. The atoms are contained in a 2.4 cm diameter spherical cell made from aluminosilicate glass filled with 9.4 amagats of ^{3}He, 29 Torr of N_2 for quenching, and a drop of K metal in the stem of the cell. The cell is heated to 185 °C by ac currents at 300 kHz in a twisted pair wire heater, maintaining K density at 7×10^{13} cm^{-3}. A separate stem heater controls the position of the K drop plugging the stem neck to preserve the spherical shape of the polarized ^{3}He. The magnetic shields consist of 3 layers of μ-metal and an inner ferrite shield to reduce thermal magnetic noise and provide an overall shielding factor of 10^8 [22]. Furthermore, a set of large Helmholtz coils surround the apparatus

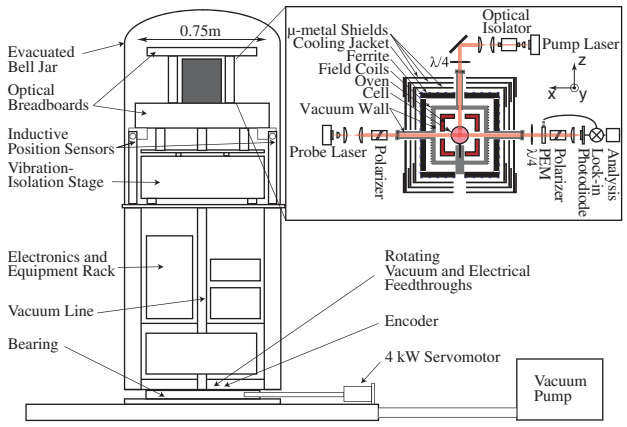

FIG. 1 (color online). Experimental setup of the rotating comagnetometer.

to cancel Earth's magnetic field and eliminate Faraday rotation in optical elements. K atoms are optically pumped in the $\hat{z}$ direction with about 10 mW of K $D1$ light generated by a distributed-feedback laser. Coils inside the magnetic shields are used to cancel residual magnetic fields and create the compensation B_z field. The polarization of K atoms in the $\hat{x}$ direction is measured using optical rotation of a 10 mW linearly polarized off-resonant probe beam generated by a distributed-feedback laser tuned to 770.76 nm. The residual magnetic fields inside the shields and the light shift due to residual probe beam circular polarization are eliminated using zeroing routines described in [17,20]. The pump beam light shift is reduced by tuning the laser to the zero light shift point on the $D1$ line and monitoring its wavelength with a Burleigh WA-1500 wave meter. The volume around the cell is evacuated to 2 mTorr and the bell jar over the entire optical setup is pumped out to 2 Torr to eliminate beam motion due to air currents. We achieve sensitivity to β_y^N, β_y^e fields of 2 fT$/\sqrt{\text{Hz}}$ at the apparatus reversal frequency of 0.023 Hz.

The optical setup and associated electronics are mounted on a rotary platform driven through a worm gear by an ac servomotor. Electric power and vacuum connections are provided by rotary feedthroughs. The experiment is controlled by a computer on the rotary platform with a wireless internet connection. A rotary encoder measures the angle of the platform and noncontact position sensors monitor the orientation of the vibration-isolation platform inside the bell jar. The tilt of the rotation axis is measured with electronic tilt sensors and zeroed to reduce laser beam motion correlated with apparatus rotation.

The comagnetometer signal as a function of the rotation angle in the lab frame is shown in Fig. 2. A large signal is observed due to the projection of the Earth's rotation onto the $\hat{y}$ direction. To remove this and other possible backgrounds fixed relative to the Earth, we measure the sidereal oscillations in the comagnetometer signal amplitude resulting from 180° reversal of the platform. We alternate either between north and south orientations or east and west

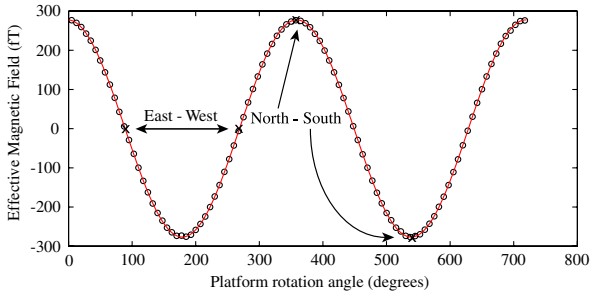

FIG. 2 (color online). Amplitude of the comagnetometer signal for a 180° rotation as a function of the initial platform rotation angle. The Lorentz violation data are collected at four points indicated by crosses.

orientations every 22 sec. The signal is recorded for 3–7 seconds while the apparatus is stationary. Fast damping of spin transients in the comagnetometer [17] is crucial for such data collection. After seven orientation reversals, a 90° rotation is performed to switch to the other heading pair, the B_z field is adjusted to the compensation point, and a sensitivity calibration is performed. From these data, we extract the reversal-correlated amplitude. Every 7 hours data collection pauses in the south position for zeroing of other magnetic field components and probe light shift. These operations are fully automated and the experiment can run for several weeks without significant intervention. Figure 3 shows the amplitude of the N-S and E-W signals as a function of the sidereal time for a long run. The amplitude of the N-S signal agrees with the projection of the Earth's rotation at our latitude within 2%, and the E-W signal is close to zero within the accuracy of the absolute orientation of the comagnetometer. In the presence of Lorentz violation, each signal would exhibit a sinusoidal variation at the sidereal frequency. We remove backgrounds slowly varying over several days and fit the data to a sum of sine and cosine signals. The error bars of the fit amplitudes are increased by the reduced χ^2 of the fit, which is typically about 4.

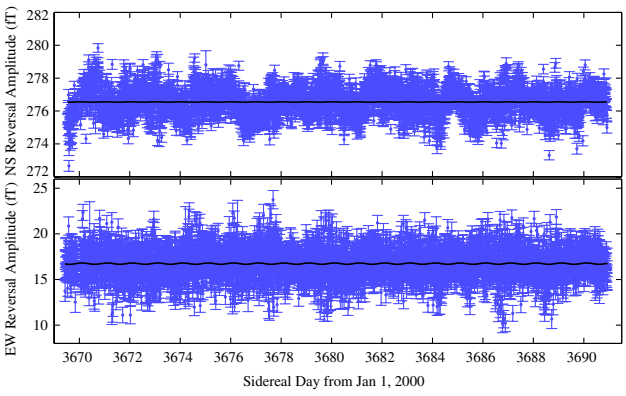

FIG. 3 (color online). Amplitude of the comagnetometer signal for N-S and E-W reversals as a function of sidereal time with a sinusoidal fit. Each data point represents seven orientation reversals.

The calibration of the comagnetometer can be performed in several ways. We usually use a calibration based on Eq. (5) of Ref. [17], which can be performed at the same time as adjustment of the B_z field. However, we found that it is sensitive to gradients in magnetic field and alkali polarization. A more accurate calibration was performed separately using slow modulation of the B_x field. A sinusoidal modulation of the B_x field at a frequency ω with amplitude B_0 generates an out-of-phase response given by

$$P_x^e = \frac{\gamma_e P_z^e}{R_{\rm tot}} \frac{\omega B_0}{\gamma_N B_z} \tag{2}$$

for $\omega \ll \gamma_N B_z$. It was verified using several other calibration methods, such as rotation of the apparatus around the vertical axis. Furthermore, the Earth's rotation rate provides an additional check of the calibration.

The data were collected for 143 days from July 2009 to April 2010 and are shown in Fig. 4. The long time span provides an important separation between sidereal and possible diurnal variations. It is also important to note that the N-S signal and the E-W signal are susceptible to different systematic effects. The N-S signal is mostly sensitive to changes in the comagnetometer sensitivity, while the E-W signal is sensitive to changes in the orientation of the apparatus and drifts in the B_z field and pump beam light shift. Furthermore, a true sidereal signal would appear out of phase in the N-S and E-W signals:

$$S_{\rm EW} = \beta_Y^N \cos(2\pi t) - \beta_X^N \sin(2\pi t) \tag{3}$$

$$S_{\rm NS} = [-\beta_X^N \cos(2\pi t) - \beta_Y^N \sin(2\pi t)] \sin\chi, \tag{4}$$

where $\chi = 40.35°$ is the latitude at Princeton, β_X^N, β_Y^N are the components of the anomalous magnetic field in the geocentric equatorial coordinate system coupling to the ^{3}He nuclear spin, and t is the local sidereal time.

A number of parameters of the experiment, such as various temperatures, pump and probe beam positions, apparatus tilt, and ambient magnetic fields were monitored, but no significant correlations with the comagnetometer signal were found. The only finite correlation was due to drifts in the pump beam light shift and was corrected for based on laser wavelength measurements. To estimate the systematic uncertainty, the data analysis was performed using several methods. For example, the first point after pausing for B_z adjustment can be eliminated because of extra scatter associated with vibration-isolation platform settling. The reversal amplitude for each series of seven 180° rotations can be extrapolated to the time of B_z adjustment to correct for drifts of ^{3}He polarization. The data can be fit separately for each 1-day interval to avoid potential bias from long-term drift removal. All these methods and their combinations gave consistent results and the scatter among them was used as a conservative estimate of the systematic error.

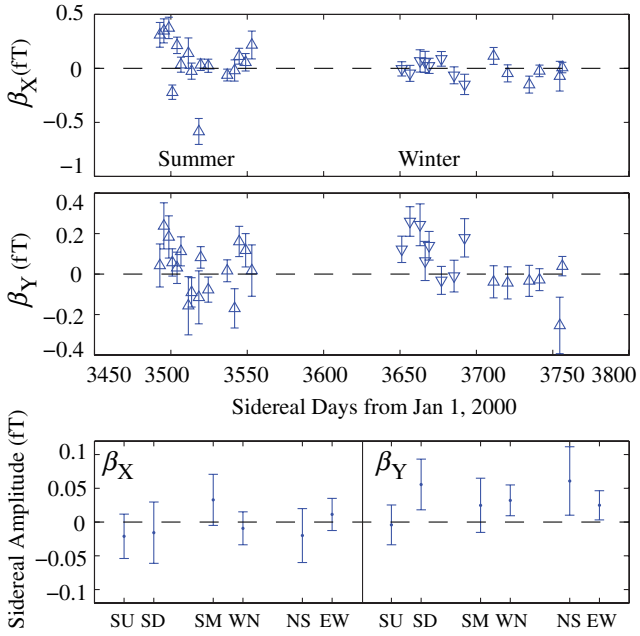

FIG. 4 (color online). Top panel: Summary of the data as a function of time. Each data point represents a several-day run. Upward and downward triangles represent direction of ^{3}He spin. Bottom panel: Systematic comparisons: SU/SD - spin up vs spin down (from winter data only), SM/WN - summer vs winter data, EW/NS - amplitudes from E-W vs N-S reversals only.

It can be seen from Fig. 4 that summer data has a larger scatter of data points than indicated by their error bars. We believe this is due to fluctuations of the background optical rotation due to small light interference effects affected by rotation of the apparatus. In the winter, we implemented additional optical background measurements for 1.5–2 sec each time the apparatus was at rest by applying a large B_z field inside the shields to suppress rotation from the atoms. Subtraction of this background from the signal reduces the scatter of the data. In obtaining the final result, the summer and winter data are averaged separately, scaling the errors by their respective χ^2 before the final average. The bottom panel of Fig. 4 shows the comparison of the results taken in the summer vs winter, with the ^{3}He spins up vs down, and obtained separately from E-W and N-S signals. It can be seen that all data subdivisions are consistent with each other.

We obtain the following final result with statistical and systematic errors:

$$\beta_X^N = (0.001 \pm 0.019 \pm 0.010)\ \text{fT} \tag{5}$$

$$\beta_Y^N = (0.032 \pm 0.019 \pm 0.010)\ \text{fT}. \tag{6}$$

In comparison, the limit on electron Lorentz violation from [9] is equivalent to a magnetic field of 0.002 fT, so we can ignore possible signal from electron interactions.

These results can be interpreted in terms of the parameters in the SME [10]. The following three- and four-dimensional operators in the relativistic Lagrangian can be constrained from coupling to a spin-1/2 particle

$$\mathcal{L} = -\bar{\psi}\left(m + b_\mu \gamma^5 \gamma^\mu + \frac{1}{2} H_{\mu\nu}\sigma^{\mu\nu}\right)\psi + \frac{1}{2} i\bar{\psi}\left(\gamma_\nu + d_{\mu\nu}\gamma^5\gamma^\mu + \frac{1}{2} g_{\lambda\mu\nu}\sigma^{\lambda\mu}\right)\overleftrightarrow{\partial}^\nu \psi. \quad (7)$$

Here b_μ and $g_{\lambda\mu\nu}$ are CPT-odd fields, while $d_{\mu\nu}$ and $H_{\mu\nu}$ are CPT-even fields. Five and six-dimensional operators can also lead to spin coupling terms [15,23]. To leading order the spin energy shift can be written as

$$\delta E = -\mu_{^3\mathrm{He}} \beta_i^N \sigma_i^N = -P_n \tilde{b}_i^n \sigma_i^n - 2P_p \tilde{b}_i^p \sigma_i^p, \quad (8)$$

where $P_n = 0.87$ and $P_p = -0.027$ are the polarizations of the neutron and protons in the ^{3}He nucleus [16] and σ_i are the Cartesian components of the spin Pauli matrix. $\tilde{b}$ is defined in terms of coefficients in Eq. (7) in Ref. [11].

Taking only the leading order neutron spin coupling, we obtain

$$\tilde{b}_X^n = (0.1 \pm 1.6) \times 10^{-33}\ \mathrm{GeV} \quad (9)$$

$$\tilde{b}_Y^n = (2.5 \pm 1.6) \times 10^{-33}\ \mathrm{GeV}, \quad (10)$$

which can be interpreted as $|\tilde{b}_\perp^n| < 3.7 \times 10^{-33}$ GeV at 68% confidence level. Our measurement is also sensitive to proton coupling $\tilde{b}_\perp^p$ at a level of 6×10^{-32} GeV and can be used in combination with the ^{3}He-^{129}Xe maser result [8] and recent analysis of the nuclear spin content of ^{129}Xe [24] to set an independent stringent limit on proton Lorentz violation. The limits on models involving higher dimension operators [13–15] and torsion [25] are also improved. The limits on boost-dependent Lorentz-and CPT-violation effects [26] can be improved from comparison of winter and summer data. Even though we measure only spatial components of spin anisotropy in the Earth's equatorial plane, timelike components of Lorentz violation could also be observed since the solar system is moving relative to the rest frame of the cosmic microwave background with a velocity $v \sim 10^{-3}c$ at a declination of $-7°$. Possible anisotropy associated with the alignment of low-order cosmic microwave background multipoles also points in approximately the same direction [27].

In conclusion, we have set a new limit on neutron spin coupling to a Lorentz- and CPT-violating background field. Our results represent a factor of 30 improvement over the previous best limit on spin anisotropy for fermions. The fundamental limits of the comagnetometer sensitivity have not yet been realized. For example, in a stationary comagnetometer we have achieved energy sensitivity of 10^{-34} GeV [18]. Additional improvements by 1–2 orders of magnitude are expected from the use of ^{21}Ne in the comagnetometer [28]. The main systematic effects are due to a combination of coupling to Earth's rotation and gravity. They can be reduced by placing the experiment near the South Pole to avoid relying on a sidereal variation for measurements of the Lorentz-violation signal. With these improvements it should be possible to achieve energy sensitivity on the order of 10^{-36} GeV, reaching the level needed to observe effects suppressed by two powers of the Planck mass, such as dimension-6 Lorentz-violating operators [23].

This work was supported by NSF Grant No. PHY-0653433 and DARPA.

[1] V. W. Hughes, H. G. Robinson, and V. Beltran-Lopez, Phys. Rev. Lett. **4**, 342 (1960).
[2] R. W. P. Drever, Philos. Mag. **6**, 683 (1961).
[3] J. D. Prestage, J. J. Bollinger, W. M. Itano, and D. J. Wineland, Phys. Rev. Lett. **54**, 2387 (1985)
[4] S. K. Lamoreaux, J. P. Jacobs, B. R. Heckel, F. J. Raab, and E. N. Fortson, Phys. Rev. Lett. **57**, 3125 (1986).
[5] P. R. Phillips, Phys. Rev. Lett. **59**, 1784 (1987).
[6] T. E. Chupp *et al.*, Phys. Rev. Lett. **63**, 1541 (1989).
[7] C. J. Berglund *et al.*, Phys. Rev. Lett. **75**, 1879 (1995).
[8] D. Bear, R. E. Stoner, R. L. Walsworth, V. A. Kostelecký, and C. D. Lane, Phys. Rev. Lett. **85**, 5038 (2000); Phys. Rev. Lett. **89**, 209902(E) (2002).
[9] B. R. Heckel *et al.*, Phys. Rev. D **78**, 092006 (2008).
[10] D. Colladay and V. A. Kostelecký, Phys. Rev. D **58**, 116002 (1998).
[11] V. A. Kostelecký and C. D. Lane, Phys. Rev. D **60**, 116010 (1999).
[12] O. W. Greenberg, Phys. Rev. Lett. **89**, 231602 (2002).
[13] R. C. Myers and M. Pospelov, Phys. Rev. Lett. **90**, 211601 (2003).
[14] I. Mocioiu, M. Pospelov, and R. Roiban, Phys. Rev. D **65**, 107702 (2002).
[15] P. A. Bolokhov, S. Groot Nibbelink, and M. Pospelov, Phys. Rev. D **72**, 015013 (2005).
[16] J. L. Friar, B. F. Gibson, G. L. Payne, A. M. Bernstein, and T. E. Chupp, Phys. Rev. C **42**, 2310 (1990).
[17] T. W. Kornack, R. K.Ghosh, and M. V. Romalis, Phys. Rev. Lett. **95**, 230801 (2005).
[18] G. Vasilakis, J. M. Brown, T. W. Kornack, and M. V. Romalis, Phys. Rev. Lett. **103**, 261801 (2009).
[19] T. W. Kornack and M. V. Romalis, Phys. Rev. Lett. **89**, 253002 (2002).
[20] T. W. Kornack, Ph.D. Dissertation, Princeton University, 2005.
[21] W. Happer and H. Tang, Phys. Rev. Lett. **31**, 273 (1973).
[22] T. W. Kornack, S. J. Smullin, S.-K. Lee, and M. V. Romalis, Appl. Phys. Lett. **90**, 223501 (2007).
[23] P. A. Bolokhov and M. Pospelov, Phys. Rev. D **77**, 025022 (2008).
[24] V. Flambaum, S. Lambert, and M. Pospelov, Phys. Rev. D **80**, 105021 (2009).
[25] V. A. Kostelecký, N. Russell, and J. D. Tasson, Phys. Rev. Lett. **100**, 111102 (2008).
[26] F. Canè *et al.*, Phys. Rev. Lett. **93**, 230801 (2004).
[27] D. J. Schwarz, G. D. Starkman, D. Huterer, and C. J. Copi, Phys. Rev. Lett. **93**, 221301 (2004).
[28] R. K. Ghosh and M. V. Romalis, Phys. Rev. A **81**, 043415 (2010).